The Development of Multifunctional Nanoparticles for Simultaneous Fluorescence Imaging and Gene Delivery

Thilini Ariyawansa

under the direction of
Dr. Mansoor M. Amiji and Mr. Mayank D. Bhavsar
Northeastern University

Research Science Institute
July 31, 2007

Abstract

Due to the controversy associated with the use of viral vectors for gene delivery, research in the use of nonviral vectors has become increasingly popular. However, these vectors are often associated with low transfection efficiencies. Recent studies have suggested that gold nanoparticles coated with the cationic polymer polyethylenimine (PEI) present an attractive solution due to the intrinsic properties of PEI. In this study, we attempt to synthesize PEI-coated gold nanoparticles which can be visualized in vivo by fluorescence microscopy. However, due to particle aggregation and high toxicity, cellular uptake and transfection efficiency of the particles was significantly impaired.

1 Introduction

Since its development, gene therapy has held great promise in the field of medicine. The ability to introduce functional genes into mammalian cells containing otherwise defective copies offers many new possibilities for the treatment of commonly acquired and inherited human diseases such as cancers, autoimmune disorders, monogenic diseases, and cardiovascular diseases [6]. The ultimate goal of gene therapy is to allow for continuous expression of transgenes in specific target tissues with minimal toxicity. Gene therapy has many benefits over other therapeutic methods; most importantly, it allows for selective treatment of the genetic defects which cause a disease in the specific cells or tissues that are effected [14].

Early applications of gene therapy allowed for efficient delivery through the use of viral vectors, taking advantage of the natural properties of viral transduction [6]. However, many of these vectors are human pathogens and thus illicit an immune response, hindering their therapeutic effects [14]. Incidences involving death as a result of the use of a viral vector for gene transfer have recently caused such methods to come under intense scrutiny [9]. These problems resulted in the development of nonviral vectors such as naked DNA and cationic liposomes, which present the additional advantages of low immunogenicity, unlimited transgene size, and the possibility of repeated administration by means of the same vector [6]. However, in spite of these advantages, nonviral vectors are often associated with low transfection effeciencies [10]. This resulted in the development of synthetic vectors, namely lipoplexes and polyplexes, which not only have a greater transfection efficiency but also prevent undesirable degradation of DNA [6].

Polyplexes are complexes of DNA and synthetic polymers, most of which are cationic and form polyplexes via electrostatic interactions with negatively-charged DNA [6]. In spite of

their appeal due to their affinity for DNA, polyplexes often present problems related to cellular uptake. Upon contact with the plasma membrane, extracellular material is invariably trapped inside endocytotic vesicles which later fuse with lysosomes. Some polyplexes are unable to facilitate the release of DNA from these compartments into the cytoplasm and thus require the presence of endosomolytic agents [6]. In addition, the complexed plasmid may not be efficiently transported across the nuclear membrane.

However, some polymers, such as polyethylenimine (PEI), possess their own method of endosome disruption, and are thus particularly attractive vectors for gene transfer [11]. Every third atom on the PEI backbone is an amino functional group, which can be protonated, resulting in a high pH buffering capacity [2]. Thus, PEI is able to trigger osmotic swelling in the endosomes, eventually resulting in their destruction and the subsequent entry of DNA into the cytoplasm [11]. Like many other cationic polymers, PEI is also very efficient in condensing DNA, further increasing its transfection efficiency [10]. Additionally, it has been shown that transfection efficiency and toxicity are strongly related to the molecular weight of PEI [7]. It is also known that conjugation to gold nanoparticles greatly increases the transfection efficiency of PEI [7]. Intravenous administration has shown that no demonstrable toxicity is effected by the nanoparticles themselves [12], suggesting an appealing combination of PEI and gold nanoparticles as a vector for gene delivery.

In the present study, we discuss the development of PEI-coated gold nanoparticles (GNPs) for the delivery of plasmid DNA into NIH3T3 murine fibroblast cells. We selected 10-kDa PEI due to its relatively high transfection efficiency and low toxicity [7]. Through layer-by-layer engineering, we created an integrated particle held together by electrostatic interactions between adjacent layers of opposite charges. Using a PEI-layer conjugated with Alexa-fluor 488, we were able to visualize the particles as they entered the cells until their destruction in

the endosome. Visualization of gene migration within the cell was facilitated by fluorescence microscopy through the use of EGFP-NI plasmid DNA.

2 Materials and Methods

2.1 Preparation of PEI-Alexa-fluor Conjugates

For the preparation of PEI-Alexa conjugates, 0.25g PEI (Polysciences, Inc, Warrington, PA, USA) and 0.0075g Alexa-fluor 488 were dissolved separately in 5ml borate buffer, pH 8.5, and incubated together for 3 hours at room temperature. The mixture was then extensively dialyzed to remove any excess Alexa-fluor molecules, and was then frozen in liquid N_2 for 5 minutes, and lyophilized to obtain a free-flowing powder.

2.2 PEI and DNA Coating of GNPs

To synthesize PEI-GNP conjugates, 1ml of 80μg/ml PEI was added to 10ml of 5mM $HAuCl_4$. This solution was added to 85ml boiling water, followed by the addition of 5ml 0.03mM sodium citrate. The solution was boiled until it became deep red in color, indicating that the particles were stabilized. The solution was left overnight at 4°C before further use. In this method of GNPs preparation, sodium citrate acts as a reducing agent on $HAuCl_4$ [16]. The negatively-charged citrate ions are later adsorbed onto the GNPs, preventing aggregation. Because PEI is a positively charged molecule, it is attracted to the GNPs, forming the particle's second layer when present in sufficient concentration.

For the DNA layer, 2μg EGFP-NI plasmid DNA (Elim Biopharmaceuticals Inc, Hayward, CA, USA) were added dropwise to 1ml PEI-GNPs, with stirring. The Au:DNA ratio was calculated to be 23.45:1μg. Following DNA coating, an 80μg/ml solution of PEI-Alexa was prepared, and 100μl were used to coat 1ml of GNPs.

2.3 GNP Characterization

Following each layer of coating, the diameter and zeta potential of the nanoparticles were measured using the 90Plus Particle Size Analyzer and the ZetaPALS software packages (Brookhaven Instruments Corporation) to ensure that the particles were of adequate size for transfection and that they had been properly coated without causing the formation of undesirable agreggations. Particle sizing was based on the principles of dynamic light scattering and measurements were made at a scattering angle of 90° [3]. The ZetaPALS software calculated zeta potential using phase analysis light scattering [4]. The zeta potential of a nanoparticle refers to the electrostatic potential created as a result of the accumulation of electrons at its surface. The ZetaPALS program calculates zeta potential using the electrophoretic mobility of the sample; the charge and intensity of the electrophoretic mobility and zeta potential are reflective of the charge and intensity of the outermost layer of the nanoparticle. Fluorescence microscopy was also used to ensure adequate Alexa-PEI coating.

2.4 Measuring DNA Loading Efficiency

The efficiency of DNA coating was measured using the PicoGreen dsDNA reagent (Molecular Probes, Eugene OR). Coated GNPs were separated from free DNA by precipitation in 20% NaCl. The PicoGreen reagent was prepared as recommended by Moleular Probes, and was incubated with the samples for 5 minutes. The fluorescence intensity was measured at 480 nm excitation and 520 nm emission, using a microplate reader.

2.5 Cytotoxicity Studies

The *in vitro* cytotoxicity of the GNPs was determined using the CellTiter 96 AQueous Non-Radioactive Cell Proliferation Assay kit (Promega Corporation, Madison, WI, USA). Approximately 10,000 NIH-3T3 mouse fibroblast cells suspended in Roswell Park Memorial

Institute media (RPMI), were seeded in each well of a 96-well plate and allowed to adhere overnight at 37 °C and 5% CO_2. The media was then replaced with 50μg/ml PEI, as a positive control, and 50μg/ml 10-kDa polyethylene glycol (PEG), as a negative control. Other wells were subjected to 80μg/ml PEI, uncoated GNPs (98.5μg/ml), GNPs with PEI (94.28μg/ml), GNPs with PEI and pDNA (approximately 94.28μg/ml), and GNPs with PEI, pDNA, and Alexa-PEI coating (90.62μg/ml). The GNP solutions were originially prepared in distilled water, lyophilized, and reconsituted in serum-free media (SFM). Incubation then continued for 6 hours, at which time the cells were replaced in SFM with the addition of 20μl of the MTS solution to each well. The cells were then incubated overnight a 37 °C and 5% CO_2. This cell viability assay is based upon the reduction of MTS, a tetrazolium salt, into a formazan compound [13]. This reduction is facilitated by reducing agents, such as NADH and NADPH, produced during oxidative phosphorylation in viable cells. As cells cannot produce the formazan product upon death, the intensity of the colored formazan is proportional to the number of viable cells. Thus, after incubation, the absorbance was read at 490 nm using a microplate reader.

2.6 In Vitro Transfection Studies

NIH-3T3 cells were seeded in six-well plates containing glass coverslips (200,000 cells per well). The cells were grown to semi-confluence at 37°C and 5% CO_2. The cells were then incubated for 24 hours under the same conditions in 180 and 90μg/ml GNPs in SFM (prepared in the same manner as for the cytotoxicity studies). After incubation, 1μg Hoechst (bisbenzimide) stain, a blue fluorescent dye, was added to each well to allow for visualization of the cell nuclei. After 15 minutes incubation with Hoechst stain, the cells were washed three times in PBS and were mounted on microscopic slides with fluorescence-free mounting media (Fluoromount-G, Southern Biotech Associates, Birmingham, AL, USA). The expression of GFP and Hoechst dye was observed using a fluorescence microscope.

2.7 Intracellular Trafficking Studies

NIH-3T3 cells were grown in 4-well chambered plates containing RPMI at 2000 cells per well. The cells were grown to semi-confluence at 37 °C and 5% CO_2. After they had reached semi-confluency, they were incubated in periods of 1 hour and 1.5 hours in 90μg/ml and 180μg/ml GNPs, and 0.1μg Hoechst stain per well. The cells were then washed three times in PBS and imaged using a Keck 3D Fusion microscope developed at Northeastern University (Boston, MA, USA). DIC and fluorescence images were taken to visualize the cellular uptake of the GNPs and their localization within the cells.

3 Results and Discussion

As the stability of the GNPs is highly dependent upon the electrostatic interactions between the different positively- and negatively-charged layers, it was important to ensure that the PEI and DNA coatings sufficiently covered the particle to produce strong positive and negative charges, respectfully. Thus, the zeta potential of the particles was calculated to ensure proper coating. The size of the particles was also measured to ensure that agreggations between particles did not form due to low PEI or DNA concentrations, as depicted schematically in Fig. 1b, shown in juxtaposition to an effectively coated particle (Fig. 1a). Proper coating results in negatively-charged GNPs are sequentially coated with postively-charged PEI, negatively-charged pDNA, and postively-charged PEI-Alexa fluor, where particles are held together through electrostatic interactions between the layers. However, as shown in Fig. 1b, low concentrations of PEI resulted in particle agreggation as more than one GNP is attracted to the same PEI molecule. This can also occur during the DNA and PEI-Alexa fluor stages of coating.

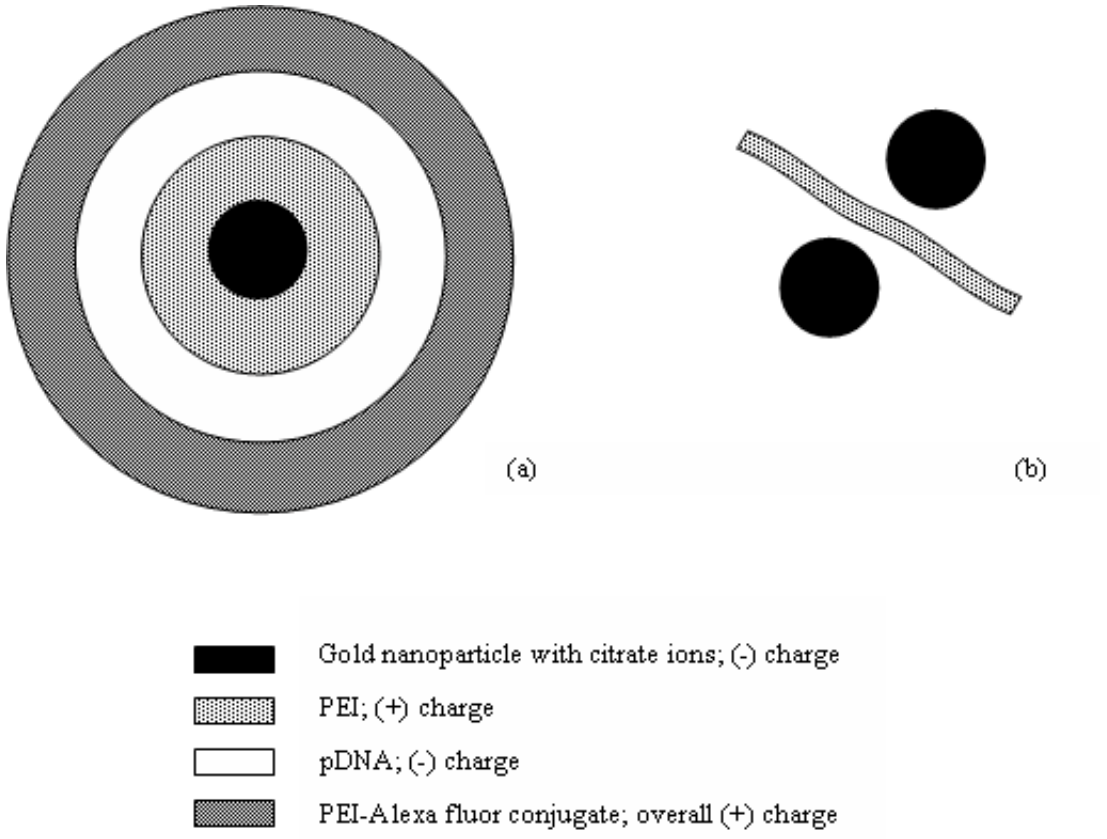

Figure 1: Effective (a) and ineffective (b) coating of GNPs. Ineffective coating results in particle aggregation.

Sample	Particle Diameter (nm)	Zeta Potential (mV)
Uncoated GNPs	48.3 ±3.7	-36.71 ±2.51
GNPs + PEI	54.6 ±2.1	-2.67 ±4.24
GNPs + PEI + pDNA	76.2 ±3.2	-20.84 ±4.60
GNPs + PEI + pDNA + Alexa-PEI	85.2 ±5.1	-13.02 ±1.59

Table 1: Mean particle sizes (nm) and zeta potentials (mV) of coated GNPs. Increases in size and changes in charge indicate adequate coating.

Although the agreggations sometimes cause changes visible to the naked eye, this is not always the case, and thus further data were collected to ensure efficient coating. The mean zeta potentials and effective diameters of the GNPs, measured following each layer of coating, the results of which are summarized in Table 1. Particle size was further clarified by transmission electron microscopy (Fig. 2).

As is expected, the uncoated GNPs are negatively charged due to the presence of citrate ions. Although the zeta potential was still negative upon addition of the first layer of PEI, it was significantly more positive than that of uncoated GNPs. After coating with DNA, the zeta potential did become more negative, indicating that successful coating had occured. This is also confirmed by the increase in particle size. Furthermore, fluorescence imaging of the nanoparticles shows that they are in fact fluorescent, confirming the coating of Alexa-PEI. However, differential interference contrast (DIC) images suggest that some of the particles have formed aggregations. Transmission electron microscopy (Fig. 2) also confirmed the particle size.

Although the particles appeared to be stable and functional in distilled water, it was clear that upon reconstitution in SFM, the particles began to aggregate. The process of lyophilization was clearly deterimental, possibly causing alternations in the GNP structure which resulted in aggregation upon resuspension. Additionally, due to high salt concentrations in

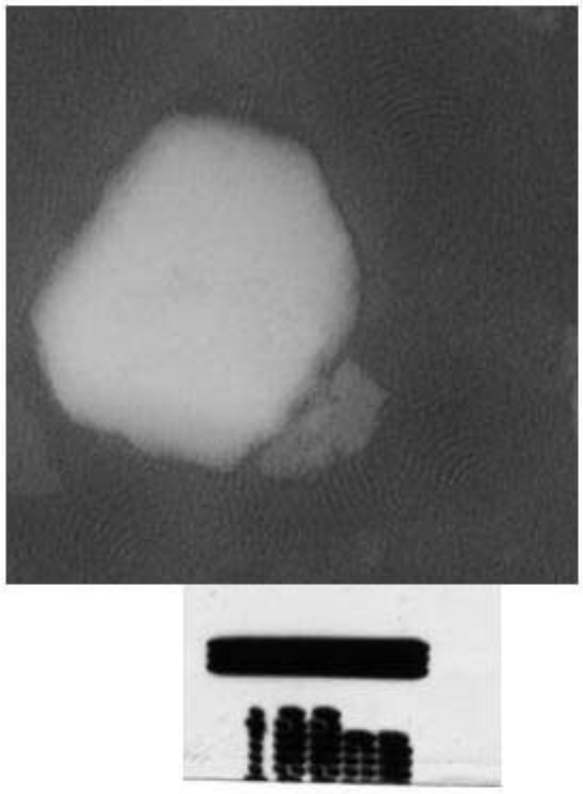

Figure 2: TEM of GNPs confirms the particle size of approximately 85nm.

SFM, it is likely that salt ions are interacting with the GNPs (which are also held together due to the alternating ionic charges of the various layers), causing further aggregation. These aggregations are clearly visible upon examination of the DIC images taken of the cell trafficking and transfection studies (Fig. 3, 5, and 7, respectively). As can be seen after 1.5 hours, and more clearly after 24 hours, of incubation, the GNPs have begun to aggregate around the cells. In addition, it appears that after 24 hours, the cells themselves have begun to form aggregations.

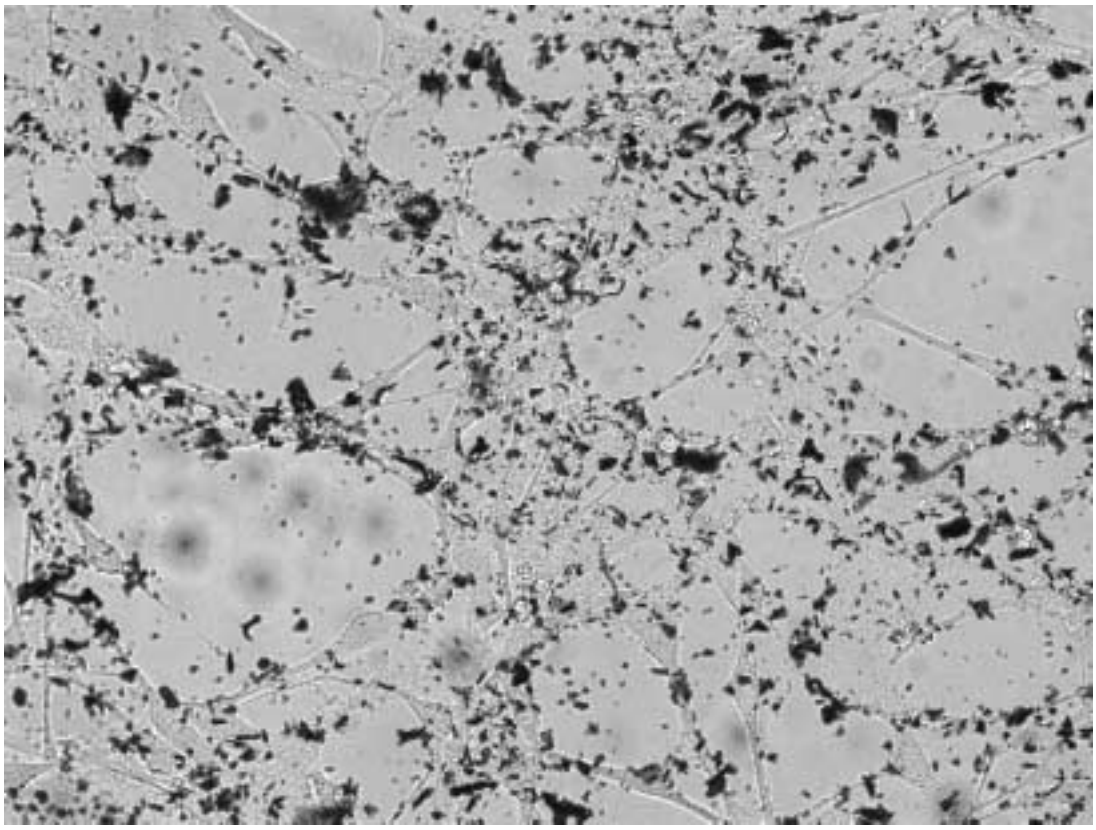

Figure 3: DIC imaging of NIH 3T3 cells after 1 hour incubation with GNPs.

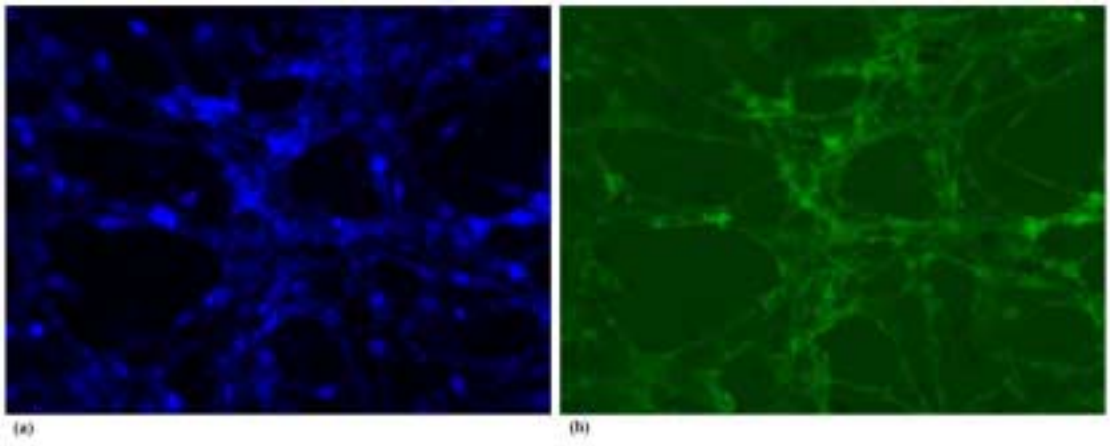

Figure 4: Fluorescence imaging of NIH 3T3 cells after 1 hour incubation with GNPs.

In spite of the aggregations, some GNPs were in fact endocytosed, as can be seen in Fig. 4 and 6. After 1.5 hours of incubation, the particles began to localize in the perinuclear region of some cells (Fig. 6). However, due to GNP aggregation, it is likely that cellular uptake was significantly decreased. It should be noted that all cell trafficking images are of cells subjected to 180μg/ml GNP, as no Alexa-fluor fluorescence was observed in cells incubated in 90μg/ml GNP.

Although there appeared to be some cellular uptake of the GNPs at 1 and 1.5 hours, significantly low levels of GFP expression were observed 24 hours post-transfection (Fig. 8). This is in spite of the fact that the PicoGreen assay revealed a 99% DNA loading efficiency. For the cells incubated in 90μg/ml GNP, only 8% of the cells (counted based upon Hoechst-stained nuclei) were found to express GFP. In the cells incubated in 180μ g/ml GNP, an even lower transfection efficiency was observed, suggesting that the higher concentration of PEI may have resulted in increased cell death.

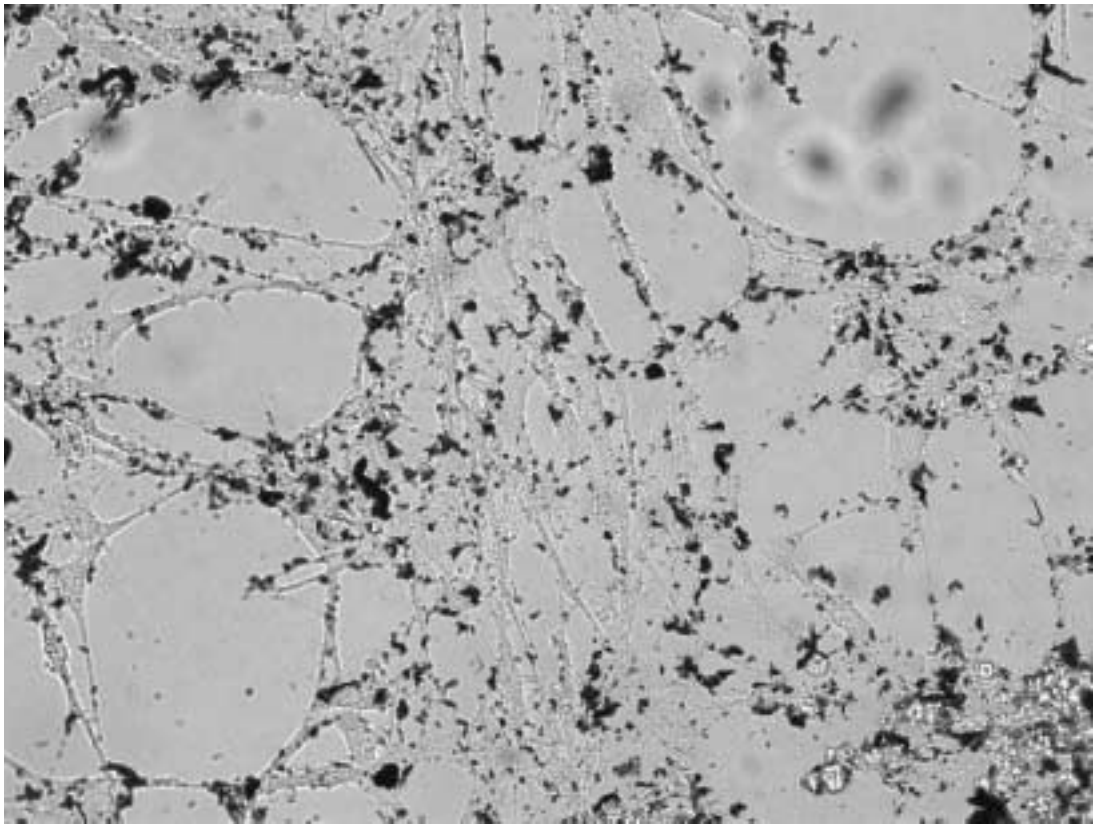

Figure 5: DIC imaging of NIH 3T3 cells after 1.5 hour incubation with GNPs. Particle aggregation on the cell membrane inhibits further cellular uptake and impairs cell viability.

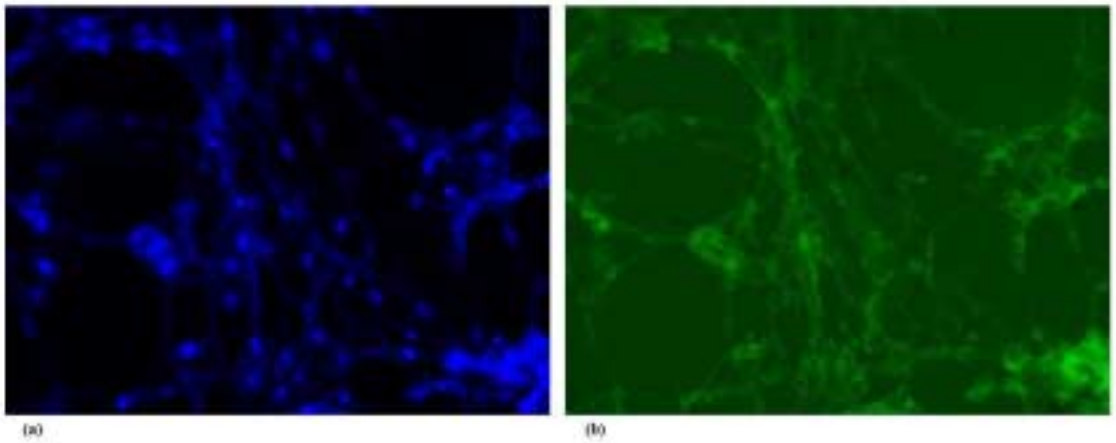

Figure 6: Fluorescence imaging of NIH 3T3 cells after 1.5 hour incubation with GNPs. In some cells, GNPs have begun to localize in the perinuclear region.

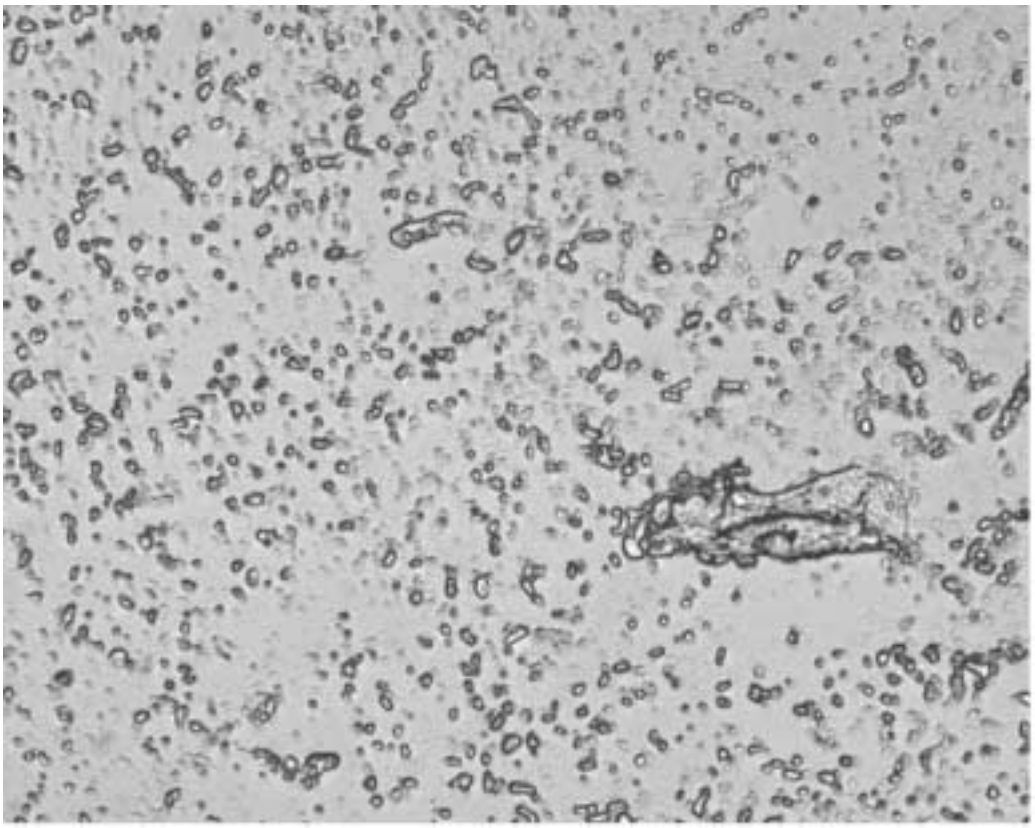

Figure 7: DIC imaging of NIH 3T3 cells after 24 hour incubation with GNPs. The combined effects of particle aggregation and toxicity lower cell viability over time.

The correlation between GNP concentration and cell death observed in the cell trafficking

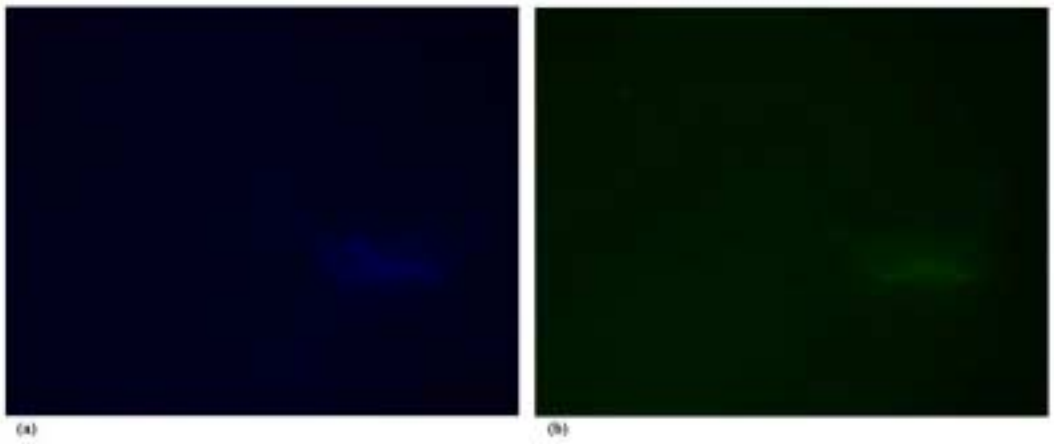

Figure 8: 24 hours post-transfection, little GFP expression is visible.

and transfection studies is further varified by the results of the cytotoxicity studies shown in Fig. 9.

The final Alexa-PEI coated GNPs showed an extremely high toxicity, resulting in approximately 26% cell viabiliy with respect to untreated cells. Considering this high toxicity of the GNPs, it is likely that the aggregated GNPs in the cell trafficking and transfection studies resulted in some cell death, which also contributed to the low expression of GFP.

4 Conclusion

PEI-coated GNPs present a promising method of gene delivery due to intrinsic properties of PEI, and in this study we demonstrated that such particles could in fact be created. However, due to problems with cytotoxicity and particle aggregation, the application of these particles was inhibited in this study. As the GNPs prepared in this study have been shown to be stable in distilled water, it is likely that lyophilization and reconsititution in SFM

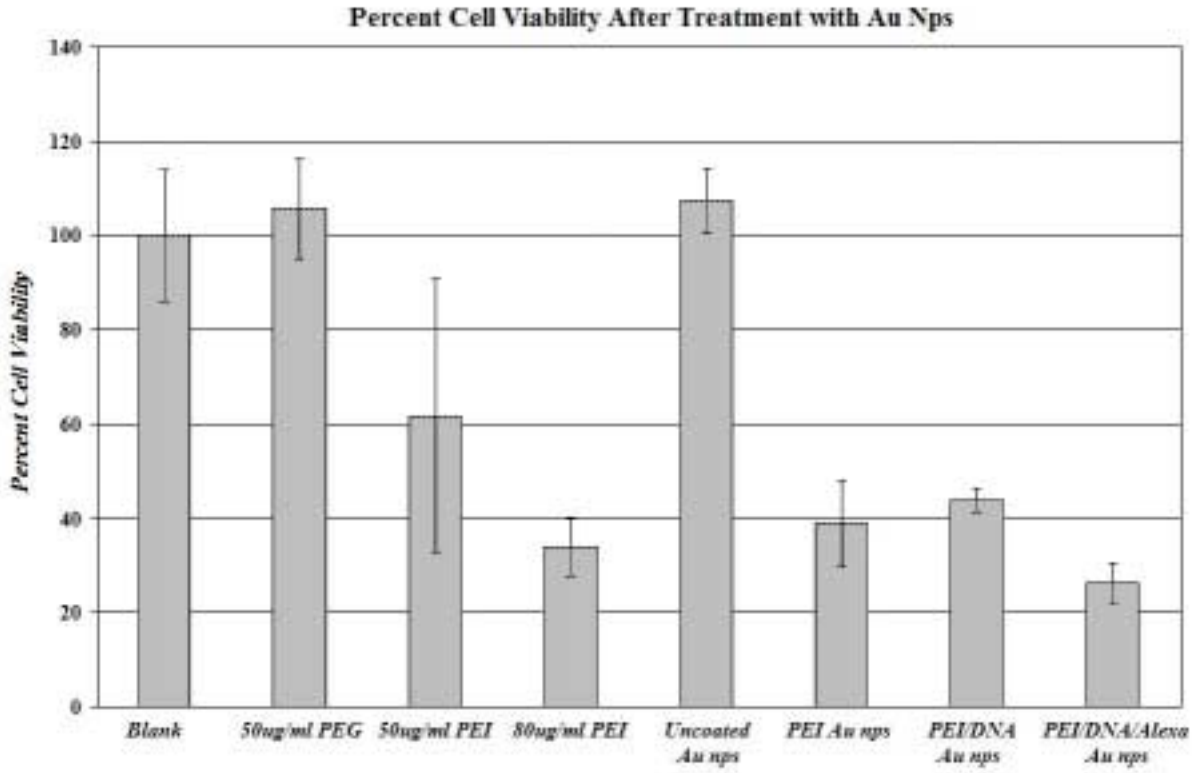

Figure 9: Percent viability of cells treated with GNP solutions. All percentages are normalized to that of the untreated cells.

are extremely detrimental to their structure, resulting in undesirable particle aggregation. This has been shown to be significantly inhibitory to cellular uptake and transfection in addition to the high toxicity of the particles prepared in this study. Thus, it is suggested that for future studies, particles be filtered or centrifuged prior to resuspension in SFM, and that different concentrations of PEI and DNA be used for coating to optimize transfection efficiency while minizing toxicity. Aggregation could also be reduced by adding a final layer of PEI conjugated to polyethylene glycol, to reduce the surface charge of the particles. In spite of the considerable cytotoxicity and aggregation problems presented by the particles developped in this study, progress has been made towards the development of functional PEI-coated GNPs that can be used for effective gene delivery

5 Acknowledgments

I would like to express my deepest gratidude to my mentor, Dr. Mansoor M. Amiji, of Northeastern University, for his help, guidance, and support throughout the course of this project. Without his valuable advice and continual motivation and encouragement I would not have completed this project. Additionally, I would like to express my thanks to Mr. Mayank D. Bhavsar and Mr. Luis Brito for their help and assistance in the laboratory. I would also like to thank Mrs. Nancy Hsia Ackerman for critical reading of this manuscript and for her constant support throughout this project. I would also like to thank the Research Science Institute for providing me with this research opportunity.

References

[1] M. D. Bhavsar, S. B. Tiwari, and M. M. Amiji. Formulation optimization for the nanoparticles-in-microsphere hybrid oral delivery system using factorial design. Journal of Controlled Release 110 (2006), no. 2, 422–430.

[2] O. Boussif, F. Lezoualc'h, M. A. Zanta, M. D. Mergny, D. Scherman, B. Demeneix, and J. Behr. A versatile vector for gene and oligonucleotide transfer into cells in culture and in vivo: Polyethylenimine. Proceedings of the National Academy of Sciences of the United States of America 92 (1995), no. 16, 7297–7301.

[3] Brookhaven Instruments Corporation. 90Plus Particle Size Analyzer. Available at `http://www.bic.com/90Plus.html` (2006/07/21).

[4] Brookhaven Instruments Corporation. ZetaPALS. Available at `http://www.bic.com/ZetaPALS.html` (2006/07/21).

[5] B. D. Chithrani, A. A. Ghazani and W. C. W. Chan. Determining the size and shape dependence of gold nanoparticle uptake into mammalian cells. Nano Letters 6 (2006), no. 4, 662–668.

[6] R. Gardlik, R. Palffy, J. Hodosy, J. Lukacs, J. Turna and P. Celec. Vectors and delivery systems in gene therapy. Medical Science Monitor 11 (2005), no. 4, 110–121.

[7] M. Thomas and A. M. Klibanov. Conjugation to gold nanoparticles enhances polyethylenimine's transfer of plasmid DNA into mammalian cells. Proceedings of the National Academy of Sciences of the United States of America 100 (2003), no. 16, 9138–9143.

[8] S. Kommareddy and M. Amiji. Preparation and evaluation of thiol-modified gelatin nanoparticles for intracellular DNA delivery in response to glutathione. Bioconjugate Chemistry 16 (2005), no. 6, 1423–1432.

[9] S. Lehrman. Virus treatment questioned after gene therapy death. Nature 401 (1999), no. 6753, 517–518.

[10] S. Li and L. Huang. Nonviral gene therapy: Promises and challenges. Gene Therapy 7 (2000), no. 1, 31–34.

[11] U. Wojda and J. L. Miller. Targeted transfer of polyethylenimine-avidin-DNA bioconjugates to hematopoietic cells using biotinylated monoclonal antibodies. Journal of Pharmaceutical Sciences 89 (2000), no. 5, 674–681.

[12] G. F. Paciotti and L. Myer. Colloidal gold: A novel nanoparticle vector for tumor directed drug delivery. Drug Delivery 11 (2004), no. 3, 169–183.

[13] T. Reiss, M. O'brien, R. Moravec, and Promega Corporation. Choosing the right cell-based assay for your research. Available at `https://promega.com/cnotes/cn006/cn006_06.pdf` (2006/07/28).

[14] G. M. Rubanyi. The future of human gene therapy. Molecular Aspects of Medicine 22 (2001), no. 3, 113–142.

[15] D. Shenoy, W. Fu, J. Li, C. Crasto, G. Jones, C. Dimarzio, S. Sridhar, and M. Amiji. Surface functionalization of gold nanoparticles using hetero-bifunctional poly(ethylene glycol) spacer for intracellular tracking and delivery. International Journal of Nanomedicine 1 (2006), no. 1, 51–57.

[16] J. Turkevich, P. C. Stevenson, and J. Hillier. The formation of colloidal gold. The Journal of Physical Chemistry 57 (1953), no. 7, 670–671.